Supporting Information

Selective urea electrosynthesis via nitrate and CO_2 reduction on uncoordinated Zn nanosheets

Experimental Section

Synthesis of Zn nanosheets

0.002 M $ZnCl_2$ and 0.03 M urea were dissolved in 50 mL deionized water with adjusting the solution pH to 5. The mixed solution was then transferred into a Teflon-lined stainless-steel autoclave which was heated at 100 ^oC for 24 h. After cooling to room temperature, the precipitates were collected by centrifugation, washed with deionized water/ethanol several times and then dried overnight. The dried precipitates were further calcined at 500 ^oC for 1 h under air atmosphere. The obtained ZnO nanosheets were then electrochemically reduced to Zn nanosheets at -0.9 V (vs RHE) in Ar-bubbled 0.5 M $NaHCO_3$ solution. The reduced products were subjected to liquid exfoliation by ultrasonication in ethanol for 2 h to obtain pristine Zn nanosheets (P-Zn). The obtained P-Zn was further subjected to Ar plasma treatment for 10 min in an AX-1000 plasma system (13.56 MHz) to obtain uncoordinated Zn nanosheets (U-Zn).

Electrochemical experiments in flow cell

Electrochemical experiments were conducted using a commercial flow cell electrolyser (101017, Gaoss Union Technology Co., LTD). A catalyst slurry was prepared by dissolving 25 mg of the catalyst in 3 mL of isopropanol and then adding 20 μL of Nafion ionomer solution (5 wt% in H_2O). Next, the catalyst slurry was slowly dropped onto the carbon paper (Sigracet 29 BC) to attain a catalyst loading of ~0.5 mg cm^{-2} as a gas diffusion electrode (GDE). Nickel mesh was used as the anode and Ag/AgCl served as the reference electrode. A proton exchange membrane (171001, Nafion N117) was used to separate the cathode and anode chambers. All potentials were referenced to a reversible hydrogen electrode (RHE) by E (V vs. RHE) = E (V vs. Ag/AgCl) + 0.198 V + 0.059 × pH. The catholyte was purged with CO_2 or Ar prior to the electrochemical experiments. During the electrolysis, CO_2 gas was fed from the no-catalyst side of the GDE at a flow rate of 20 s.c.c.m., and both catholyte and anolyte were continuously cycled at a rate of 20 mL min^{-1} under pump drive.

Electrochemical experiments in H-type cell

In H–type cell, the carbon paper–loaded catalyst (0.5 mg cm^{-2}), Pt foil and Ag/AgCl were used as the working, counter and reference electrodes, respectively. The electrolyte is consistent with the solution in the flow cell. The catholyte was purged with CO_2 or Ar prior to electrochemical experiments. During the electrolysis, a flow of CO_2 with a rate of 20 s.c.c.m. was continuously fed in the catholyte. After electrolysis at specified potentials for 1 h, the produced urea was quantitatively determined by the urease decomposition method.

Determination of urea

Urea concentration was detected via urease decomposition method[1]. Typically, 0.2 mL of urease solution with concentration of 5 mg mL^{-1} was added into 2 mL of urea electrolyte, and then reacted at 37℃ in constant temperature shaker for 40 min. Urea was decomposed by urease into CO_2 and two NH_3 molecules. After the decomposition, NH_3 concentration of urea electrolyte with urease (c_{urease}) was detected via above indophenol blue method. Meanwhile, NH_3 concentration contained in urea electrolyte without urease (c_{NH3}) was also quantified by indophenol blue method. Urea concentration (c_{urea}) in electrolyte were calculated by the following equation:

$$c_{urea} = (c_{urease} - c_{NH3})/2 \quad (1)$$

The urea yield rate and FE_{urea} were calculated by the following equation:

$$\text{Urea yield rate} = (c_{urea} \times V) / (60.06 \times t \times m) \quad (2)$$

$$FE_{urea}\ (\%) = (12 \times F \times c \times V) / (60.06 \times Q) \times 100\% \quad (3)$$

where c_{urea} (mg mL^{-1}) is the measured urea concentration, V (mL) is the volume of the electrolyte, t (h) is the reduction time, m (mg) is the catalyst loadings, F (96500 C mol^{-1}) is the Faraday constant, Q (C) is the quantity of applied electricity.

The generated NH_3 was determined by the indophenol blue method[2] and the generated NO_2^- in electrolyte was determined by a Griess test[3].

Characterizations

X-ray diffraction (XRD) pattern was collected on a Rigaku D/max 2400 diffractometer with Cu Kα radiation (λ =1.5418 Å, 40 kV). Transmission electron

microscopy (TEM) and high-resolution transmission electron microscopy (HRTEM) were performed on a Tecnai G^2 F20 microscope. Online differential electrochemical mass spectrometry (DEMS, QAS 100) was performed by QAS 100 spectrometer. Various products during the electrolysis reactions were monitored at different values of m/z signals.

Calculation details

Spin-polarized density functional theory (DFT) calculations were carried out using the Cambridge sequential total energy package (CASTEP) with projector augmented wave pseudopotentials. The Perdew-Burke-Ernzerhof (PBE) generalized gradient approximation (GGA) functional was used for the exchange-correlation potential. The van der Waals interaction was described by using the empirical correction in Grimme's scheme (DFT+D). During the geometry optimization, the electron wave functions were expanded using plane waves with a cutoff energy of 400 eV. The convergence tolerance was set to be 1.0×10^{-5} eV for energy and 0.02 eV $Å^{-1}$ for force. The 3 × 3 × 1 Monkhorst-Pack mesh was used in Brillouin zone sampling. U-Zn (101) was modeled by 4 × 4 supercell (removing one surface Zn atom), and a vacuum region of 15 Å was used to separate adjacent slabs.

The computational hydrogen electrode (CHE) model was adopted to calculate the Gibbs free energy change (ΔG) for each elementary step as follows:

$$\Delta G = \Delta E + \Delta E_{ZPE} - T\Delta S \quad (4)$$

where ΔE represents the electronic energy contribution directly derived from DFT calculations. ΔEZPE and $T\Delta S$ denote the contributions of zero-point energy and entropy (at 298.15 K), respectively. These values can be obtained from the NIST database for free molecules.

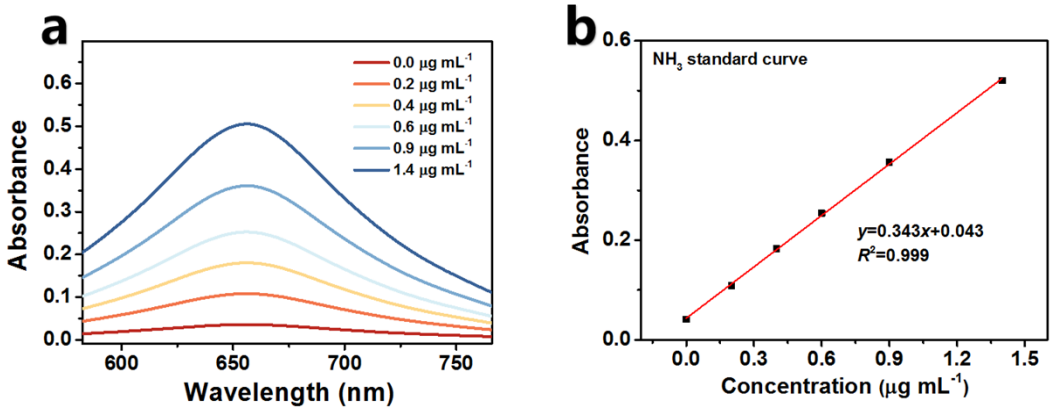

Fig. S1. (a) UV-vis absorption spectra of NH_4Cl assays after incubated for 2 h at ambient conditions. (b) Calibration curve used for the calculation of NH_3 concentrations.

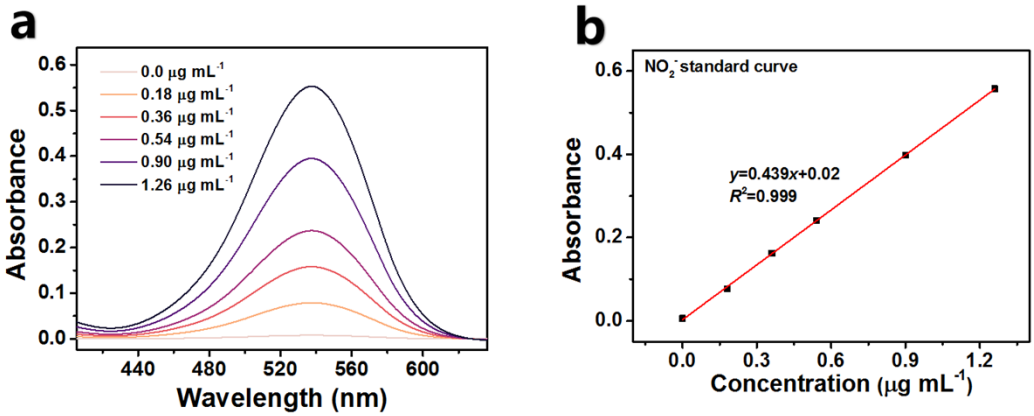

Fig. S2. (a) UV-vis absorption spectra of NO_2^- assays after incubated for 20 min at ambient conditions. (b) Calibration curve used for calculation of NO_2^- concentrations.

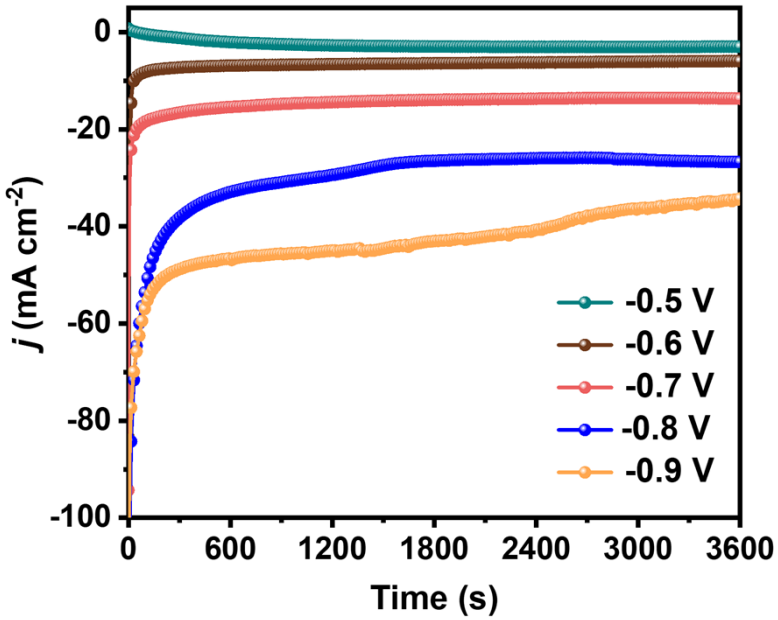

Fig. S3. Chronoamperometry curves of U-Zn at different potentials after 1 h of ENCU electrolysis.

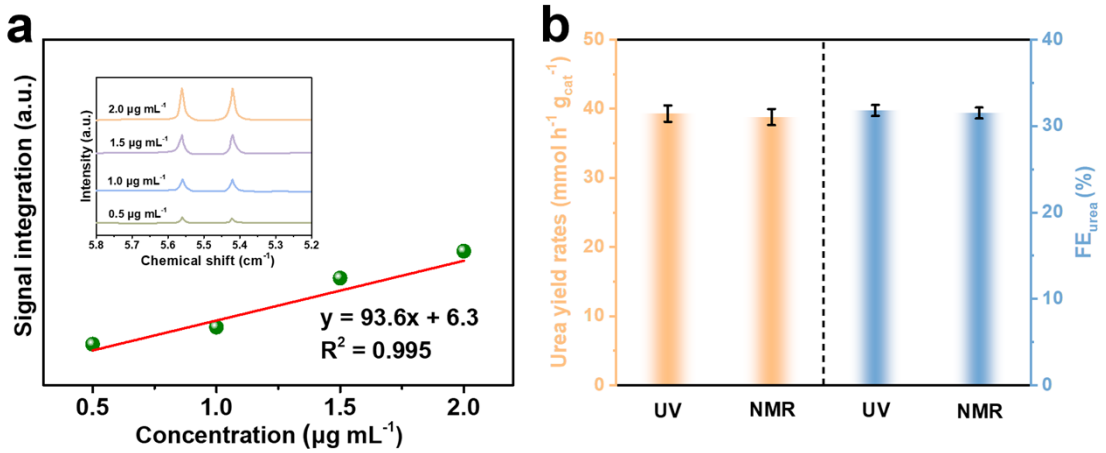

Fig. S4. (a) ^{1}H NMR spectra of $CO(^{15}NH_2)_2$ standard samples with different concentrations and corresponding calibration curves. (b) Comparison of the electrocatalytic EUCN performance of U-Zn between UV-vis and ^{1}H NMR methods at -0.8 V.

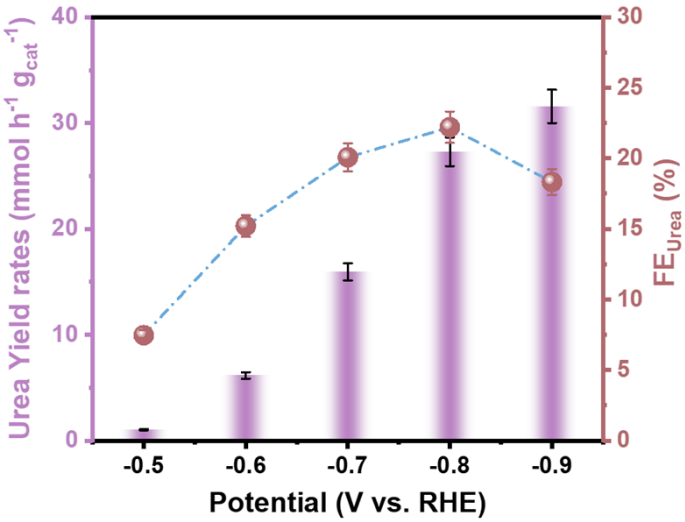

Fig. S5. Urea yield rates and FE_{urea} of U-Zn at various potentials in H-type cell.

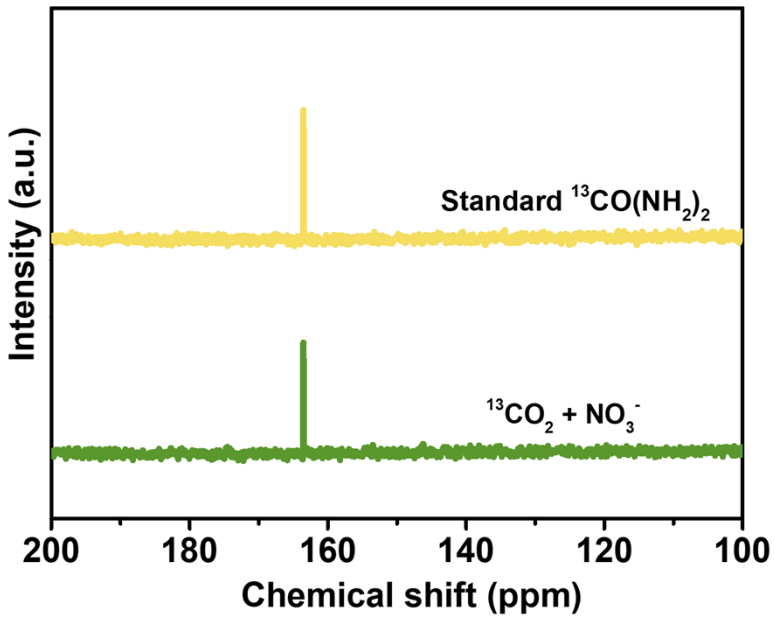

Fig. S6. ^{13}C NMR spectra of $^{13}CO(NH_2)_2$ standard sample and those fed by $^{13}CO_2$ after electrolysis at -0.8 V.

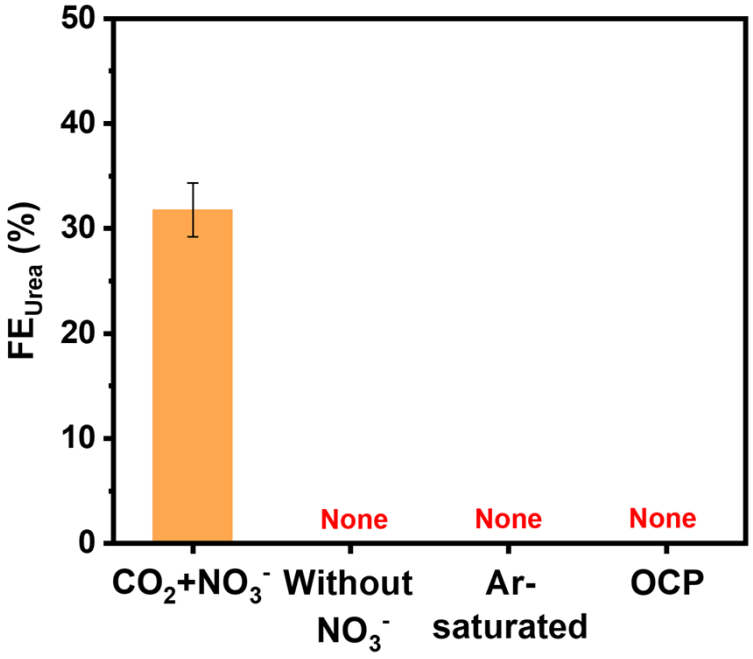

Fig. S7. Amounts of produced urea on U-Zn under different electrolysis conditions: 1) in NO_3^-/CO_2-containing solution, 2) without adding NO_3^-, 3) Ar-saturated solution, 4) open-circuit potential (OCP).

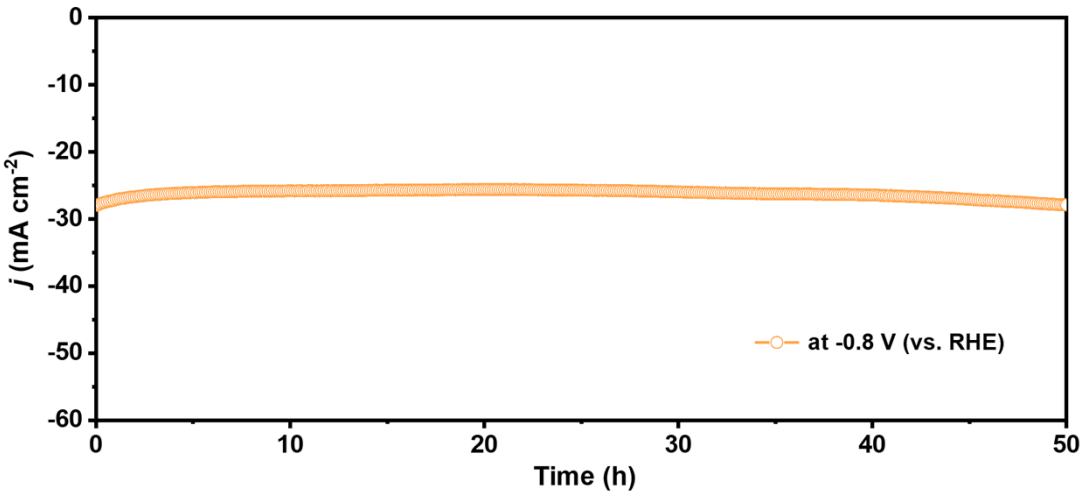

Fig. S8. Long-term stability test of U-Zn for 50 h electrolysis.

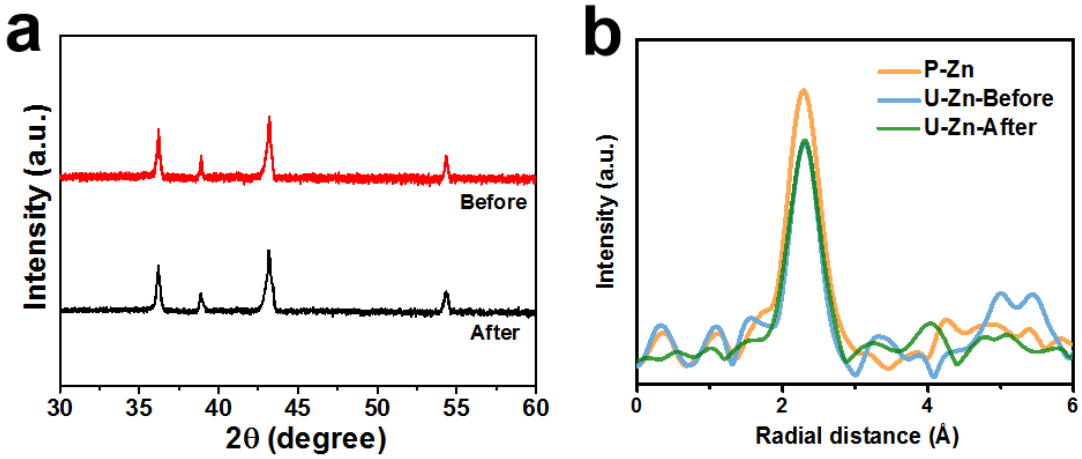

Fig. S9. Characterizations of U-Zn before and after EUCN electrolysis: (a) XRD pattern and (b) EXAFS spectra.

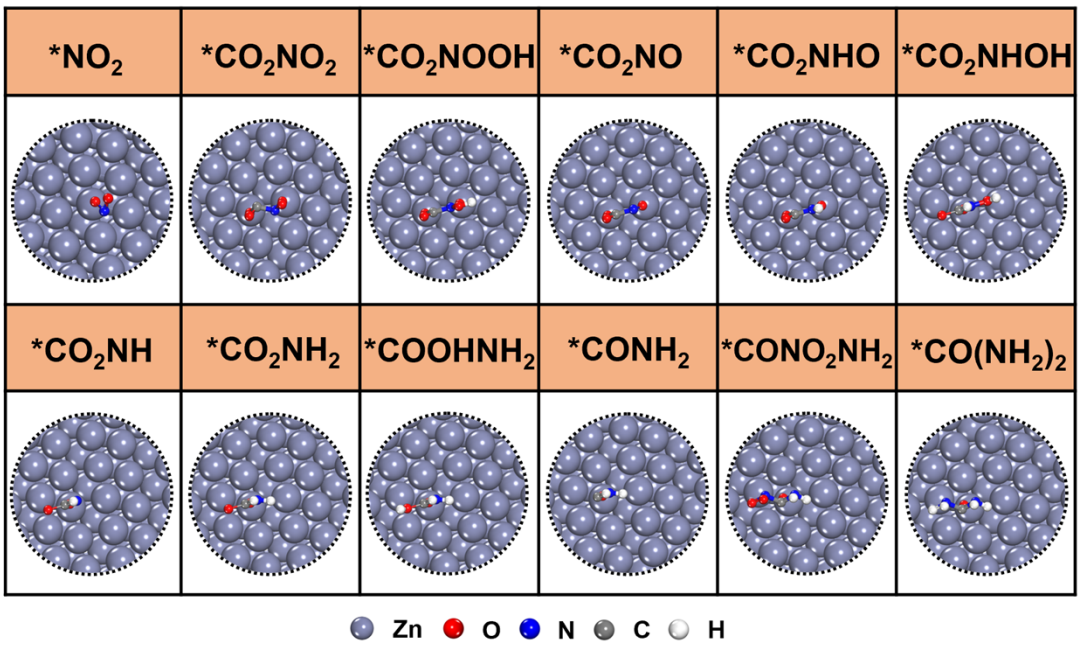

Fig. S10. Optimized atomic configurations of the reaction intermediates on P-Zn.

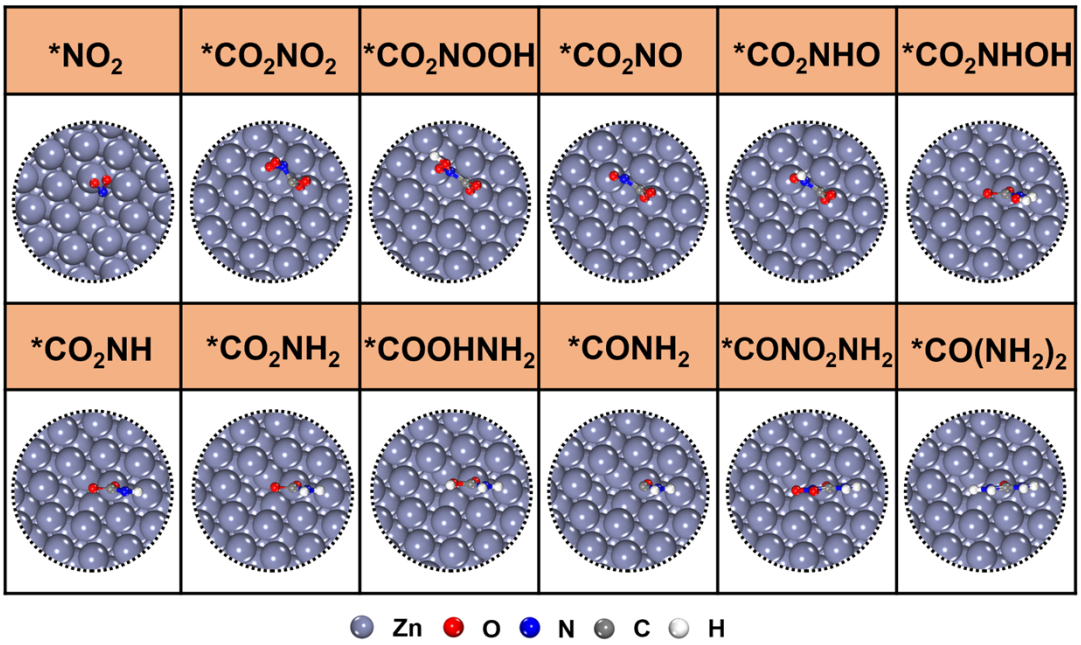

Fig. S11. Optimized structures of the reaction intermediates on U-Zn.

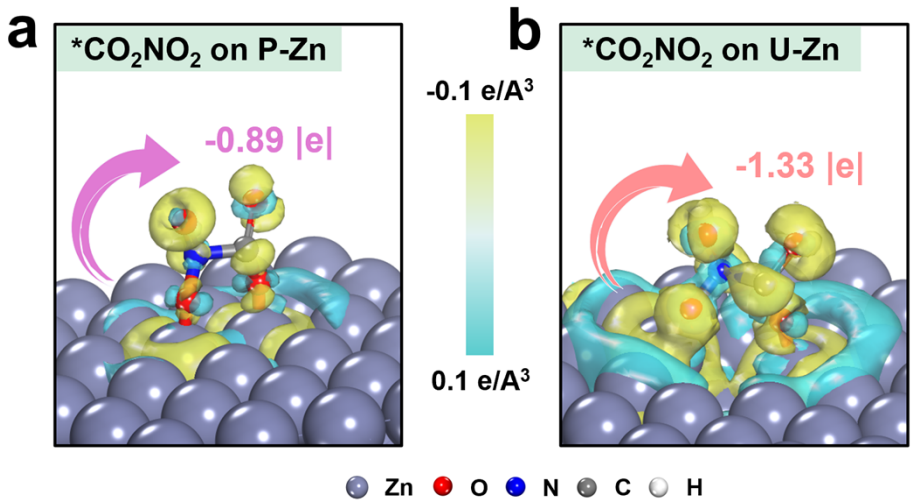

Fig. S12. EDD maps of *CO_2NO_2 on (a) P-Zn and (b) U-Zn.

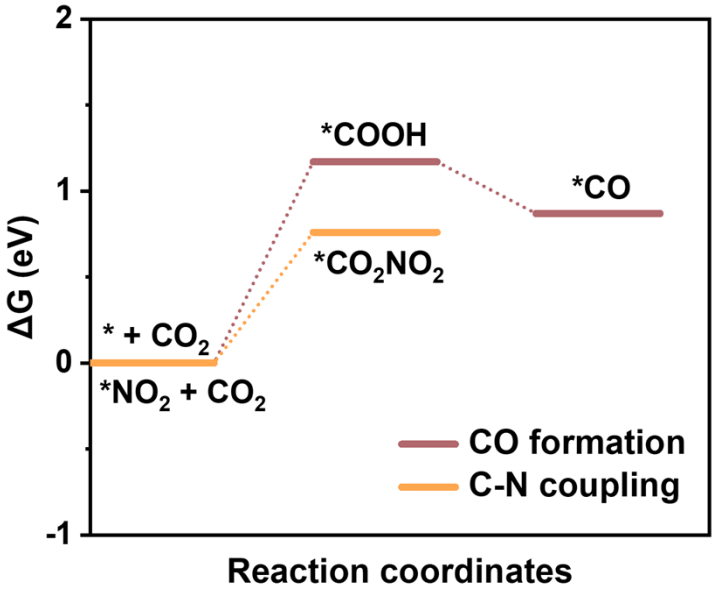

Fig. S13. Free energy profiles of $*CO_2$ reduction to form *CO and $*NO_2/CO_2$ coupling to form $*CO_2NO_2$ on U-Zn.

Table S1. Comparison of the optimum urea yield rate and FE_{urea} for the recently reported state-of-the-art EUCN catalysts at ambient conditions.

Catalyst	N/C sources	Electrolyte	Urea yield rate (mmol h^{-1} g_{cat}^{-1})	FE_{urea}	Potential (V vs. RHE)	Ref.
$In(OH)_3$−S	NO_3^-+CO_2	0.1 M KNO_3	8.88	53.4%	-0.6	4
V_O-InOOH	NO_3^-+CO_2	0.1 M KNO_3	9.87	51%	-0.5	5
Fe-Ni	NO_3^-+CO_2	0.05 M KNO_3 + 0.1 M $KHCO_3$	20.2	17.8%	-1.5	6
Cu SACs	NO_3^-+CO_2	0.1 M KNO_3 +0.1 M $KHCO_3$	29.97	28%	-0.9	7
F−CNT	NO_2^-+CO_2	0.1 M KNO_3	6.36	18%	−0.65	8
Cu−TiO_{2-x}	NO_2^-+CO_2	0.02 M KNO_2 +0.2 M $KHCO_3$	20.8	43.1%	−0.4	9
MoO_x/C	NO_3^-+CO_2	0.1 M KNO_3	23.83	27.7%	-0.6	10
m−Cu_2O	NO_2^-+CO_2	0.01 M $NaNO_3$ + 0.1 M $KHCO_3$	29.2	9.43%	-1.3	11
$FeNi_3$	NO_3^-+CO_2	0.1 M KNO_3	8.27	16.58%	−0.9	12
U-Zn	**NO_3^-+CO_2**	**0.1 M KNO_3 +0.1 M $KHCO_3$**	**27.3 (H-cell)** **39.3 (Flow-cell)**	**22.2% (H-cell)** **31.8% (Flow-cell)**	**-0.8** **-0.8**	**This Work**

Supplementary references

1. X. Wei, X. Wen, Y. Liu, C. Chen, C. Xie, D. Wang, M. Qiu, N. He, P. Zhou, W. Chen, J. Cheng, H. Lin, J. Jia, X.-Z. Fu and S. Wang, *J. Am. Chem. Soc.*, 2022, **144**, 11530-11535.
2. P. Li, Z. Jin, Z. Fang and G. Yu, *Energy Environ. Sci.*, 2021, **14**, 3522-3531.
3. Z.-Y. Wu, M. Karamad, X. Yong, Q. Huang, D. A. Cullen, P. Zhu, C. Xia, Q. Xiao, M. Shakouri, F.-Y. Chen, J. Y. Kim, Y. Xia, K. Heck, Y. Hu, M. S. Wong, Q. Li, I. Gates, S. Siahrostami and H. Wang, *Nat. Commun.*, 2021, **12**, 2870.
4. C. Lv, L. Zhong, H. Liu, Z. Fang, C. Yan, M. Chen, Y. Kong, C. Lee, D. Liu, S. Li, J. Liu, L. Song, G. Chen, Q. Yan and G. Yu, *Nat. Sustain.*, 2021, **4**, 868-876.
5. C. Lv, C. Lee, L. Zhong, H. Liu, J. Liu, L. Yang, C. Yan, W. Yu, H. H. Hng, Z. Qi, L. Song, S. Li, K. P. Loh, Q. Yan and G. Yu, *ACS Nano*, 2022, **16**, 8213-8222.
6. X. Zhang, X. Zhu, S. Bo, C. Chen, M. Qiu, X. Wei, N. He, C. Xie, W. Chen, J. Zheng, P. Chen, S. P. Jiang, Y. Li, Q. Liu and S. Wang, *Nat. Commun.*, 2022, **13**, 5337.
7. J. Leverett, T. Tran-Phu, J. A. Yuwono, P. Kumar, C. Kim, Q. Zhai, C. Han, J. Qu, J. Cairney, A. N. Simonov, R. K. Hocking, L. Dai, R. Daiyan and R. Amal, *Adv. Energy Mater.*, 2022, **12**, 2201500.
8. X. Liu, P. V. Kumar, Q. Chen, L. Zhao, F. Ye, X. Ma, D. Liu, X. Chen, L. Dai and C. Hu, *Appl. Catal. B*, 2022, **316**, 121618.
9. N. Cao, Y. Quan, A. Guan, C. Yang, Y. Ji, L. Zhang and G. Zheng, *J. Colloid Interface Sci.*, 2020, **577**, 109-114.
10. M. Sun, G. Wu, J. Jiang, Y. Yang, A. Du, L. Dai, X. Mao and Q. Qin, *Angew. Chem. Int. Edit.*, 2023, **62**, e202301957.
11. M. Qiu, X. Zhu, S. Bo, K. Cheng, N. He, K. Gu, D. Song, C. Chen, X. Wei, D. Wang, Y. Liu, S. Li, X. Tu, Y. Li, Q. Liu, C. Li and S. Wang, *CCS Chem.*, 2023, **5**, 2617-2627.
12. T. Hou, J. Ding, H. Zhang, S. Chen, Q. Liu, J. Luo and X. Liu, *Mater. Chem. Front.*, 2023, **7**, 4952-4960.